

# A lattice determination of QCD field strength correlators

Gunnar S. Bali

*Department of Physics, The University of Southampton,  
Highfield, Southampton SO17 1BJ, England*

Nora Brambilla<sup>1 \*</sup> and Antonio Vairo<sup>1</sup>

*Institut für Theoretische Physik, Universität Heidelberg  
Philosophenweg 16, D-69120 Heidelberg, FRG*

*\* INFN, Sezione di Milano, Via Celoria 16, 20133 Milano, Italy*

---

## Abstract

We study field strength correlators in presence of a static quark-antiquark pair by use of lattice methods. The lattice data have been acquired recently in the context of a determination of relativistic corrections to the static interquark potential. We extract independent estimates of the form factors of two point correlation functions and investigate the effect of higher order correlators. Our results confirm the dominance of the two point correlators in the regions of intermediate and large quark separations, and are compatible with correlation length values obtained from different approaches.

---

---

<sup>1</sup> Alexander von Humboldt Fellow

## 1 Introduction

Understanding the QCD dynamics requires insight into non-trivial QCD vacuum properties. In their pioneering work, Shifman, Vainshtein and Zakharov [1] focused on implications of condensation of quarks and gluons onto elementary particle spectroscopy. Soon, it emerged that in general not only the condensates had to be considered but also the space-time dependence of correlation functions as well as a correlation length [2]. Since then, lattice studies concentrated on the measurement of the gauge invariant field strength correlator

$$g^2 \langle \phi(0, x) F_{\mu\nu}(x) \phi(x, 0) F_{\lambda\rho}(0) \rangle, \quad (1)$$

$$F_{\mu\nu} = T^a F_{\mu\nu}^a, \quad A_\mu = T^a A_\mu^a, \quad \phi(x, 0) = P \exp \left\{ ig \int_x^0 dz_\mu A_\mu(z) \right\},$$

which, at large distances, exhibits an exponential fall-off behaviour that is controlled by a correlation length  $\lambda_g$ . The Stochastic Vacuum Model (SVM) offers a systematic way to treat non-perturbative QCD effects which enter in terms of gluon field strength correlation functions [3]. In this approach a picture emerges in which the correlator (1) plays a basic role in understanding colour confinement. It can be decomposed in terms of two form factors  $D$  and  $D_1$ ,

$$\begin{aligned} g^2 \langle \phi(0, x) F_{\mu\nu}(x) \phi(x, 0) F_{\lambda\rho}(0) \rangle = & \\ & \frac{g^2 \langle F^2(0) \rangle}{24N_c(D(0) + D_1(0))} \left\{ (\delta_{\mu\lambda}\delta_{\nu\rho} - \delta_{\mu\rho}\delta_{\nu\lambda})(D(x^2) + D_1(x^2)) \right. \\ & \left. + (x_\mu x_\lambda \delta_{\nu\rho} - x_\mu x_\rho \delta_{\nu\lambda} + x_\nu x_\rho \delta_{\mu\lambda} - x_\nu x_\lambda \delta_{\mu\rho}) \frac{d}{dx^2} D_1(x^2) \right\}. \end{aligned} \quad (2)$$

All parameters within the SVM can in principle be derived in a lattice simulation directly from the QCD Lagrangian. The simplest linkage between the analytic model and lattice gauge theory can be found in the Gaussian approximation to the SVM. In this approximation cumulants of order higher than two in the field strength are neglected in the Wilson loop, such that it is sufficient to evaluate two-point correlation functions on the lattice. Within this approximation, successful predictions ranging from the colour electric field distribution within the QCD flux tube between two static quarks and the determination of the QCD static potential to high energy hadron scattering [4] have been produced. To our knowledge all previous lattice evaluations of field strength correlators have concentrated on determining two point correlators only (see however [5] for an attempt of incorporating higher order effects) and relied on Eq. (2) in the simplest choice of the Schwinger line factors in

connection with the cooling method [6].

In this paper we have chosen a different approach. We investigate effects of field strength correlators in presence of a static  $q\bar{q}$  pair to all orders; these in principle contain all physical information about the flux tube configuration and the  $q\bar{q}$  heavy quark confined system. With the techniques developed in the Wilson loop approach (i.e. manifestly gauge-invariant approach to quark dynamics) the complete gauge-invariant quark-antiquark potential at order  $1/m^2$  in the quark mass can be obtained from such field strength correlators [7,8]. Recently, these analytic expressions were used to obtain the complete semirelativistic potential from the lattice [9]. Subsequently, the experimental bottomonium spectrum has been fitted to these QCD predictions, and a lattice scale as well as the bottom quark mass have been obtained.

Within the present study, we will use the same (lattice) correlation functions 1) to investigate the importance of higher order correlation functions within the range of interquark distances realized ( $\sim 0.1\text{--}1$  fm) and 2) to extract in this accessible region the behaviour of the  $D$  and  $D_1$  functions. Therefore, we do not only aim at a consistency check of the approximation involved in the definition of the Gaussian Stochastic Vacuum Model but demonstrate indirectly the impact of these non-perturbative correlators onto quarkonia spectra.

The paper is organized as follows. In Sec. 2 we introduce the vacuum expectation values that have been evaluated on the lattice and their relation to the Wilson loop (and therefore to the potential). Furthermore, we outline the strategy adopted to identify the contribution of the higher order correlators; in Sec. 3 we discuss the numerical results, the validity of the Gaussian approximation in the SVM and try to extract the large  $r$  behaviour of the  $D$  and  $D_1$  form factors before we present our conclusions in Sec. 4.

## 2 Wilson loop and field strength correlation functions

Given a set of Schwinger lines  $\Phi \equiv \{\phi(0, u) = \exp\{ig \int_0^u dz_\mu A_\mu(z)\}, \quad u \in E\}$ , connecting points  $u$  in Euclidean space  $E$  with the origin 0 of the reference frame, the Wilson loop  $\langle W(\Gamma) \rangle \equiv \langle \exp\{ig \oint_\Gamma dz_\mu A_\mu(z)\} \rangle$  can be expanded as [3,10],

$$\begin{aligned} \log \langle W(\Gamma) \rangle &= \sum_{n=0}^{\infty} \frac{(ig)^n}{n!} \int_{S(\Gamma)} dS_{\mu_1 \nu_1}(u_1) \cdots dS_{\mu_n \nu_n}(u_n) \langle \phi(0, u_1) \\ &\quad \times F_{\mu_1 \nu_1}(u_1) \phi(u_1, 0) \cdots \phi(0, u_n) F_{\mu_n \nu_n}(u_n) \phi(u_n, 0) \rangle_{\text{cum}}. \end{aligned} \quad (3)$$

$S(\Gamma)$  denotes a surface with contour  $\Gamma$ .<sup>2</sup> The cumulants  $\langle \cdot \rangle_{\text{cum}}$  are defined in terms of path integral averages over gauge fields,

$$\begin{aligned} \langle \phi(0, u_1) F(u_1) \phi(u_1, 0) \rangle_{\text{cum}} &= \langle \phi(0, u_1) F(u_1) \phi(u_1, 0) \rangle, \\ \langle \phi(0, u_1) F(u_1) \phi(u_1, u_2) F(u_2) \phi(u_2, 0) \rangle_{\text{cum}} &= \\ &\quad \langle \phi(0, u_1) F(u_1) \phi(u_1, u_2) F(u_2) \phi(u_2, 0) \rangle \\ &\quad - \langle \phi(0, u_1) F(u_1) \phi(u_1, 0) \rangle \langle \phi(0, u_2) F(u_2) \phi(u_2, 0) \rangle, \\ &\quad \dots \quad \dots \end{aligned}$$

where  $\phi(u_1, u_2) \equiv \phi(u_1, 0) \phi(0, u_2)$  is a shorthand notation. Notice that since the left-hand side of Eq. (3) is independent of the set of paths  $\Phi$  as well as of the choice of the surface  $S$ , all these dependencies are expected to cancel out after summation of the whole series. However, in general, each cumulant appearing within the right-hand side will depend on the choice of  $\Phi$ .

Let us define

$$\mathcal{F}_{\mu\nu\lambda\rho}(x; \Gamma) \equiv \langle\langle g^2 F_{\mu\nu}(x) F_{\lambda\rho}(0) \rangle\rangle_{\Gamma} - \langle\langle g F_{\mu\nu}(x) \rangle\rangle_{\Gamma} \langle\langle g F_{\lambda\rho}(0) \rangle\rangle_{\Gamma}. \quad (4)$$

This object is required to compute the  $1/m^2$  corrections to the static interquark potential [7,8]. The double bracket  $\langle\langle \cdot \rangle\rangle_{\Gamma}$  stands for the average over gauge fields in presence of the Wilson loop  $W(\Gamma)$

$$\langle\langle \cdot \rangle\rangle_{\Gamma} \equiv \frac{\langle \cdot W(\Gamma) \rangle}{\langle W(\Gamma) \rangle};$$

from now on we will assume that the points  $x \equiv (\mathbf{r}, t)$  and 0 belong to the first and second temporal quark line, respectively (see Fig. 1).

Some particular cases are ( $E_i = F_{i4}$ ,  $B_i = \epsilon_{ijk} F_{jk}/2$ ):

$$\begin{aligned} \mathcal{E}(x; \Gamma) &\equiv \mathcal{F}_{i4i4}(x; \Gamma) = \langle\langle \mathbf{E}(x) \cdot \mathbf{E}(0) \rangle\rangle_{\Gamma} - \langle\langle \mathbf{E}(x) \rangle\rangle_{\Gamma} \cdot \langle\langle \mathbf{E}(0) \rangle\rangle_{\Gamma}, \\ \mathcal{B}(x; \Gamma) &\equiv \frac{1}{4} \epsilon_{ilm} \epsilon_{ijk} \mathcal{F}_{lmjk}(x; \Gamma) = \langle\langle \mathbf{B}(x) \cdot \mathbf{B}(0) \rangle\rangle_{\Gamma}, \\ \mathcal{C}(x; \Gamma) &\equiv \frac{1}{2} \epsilon_{ijk} \mathcal{F}_{i4jk}(x; \Gamma) = \langle\langle \mathbf{E}(x) \cdot \mathbf{B}(0) \rangle\rangle_{\Gamma} \end{aligned}$$

<sup>2</sup> Until now it has not been completely proven that the series Eq. (3) has a finite convergence radius. We assume that with our choice of  $\Phi$  a region of convergence exists.

$$\begin{aligned}
&= \frac{1}{2} \epsilon_{ijk} \mathcal{F}_{jk i4}(x; \Gamma) = \langle\langle \mathbf{B}(x) \cdot \mathbf{E}(0) \rangle\rangle_{\Gamma}, \\
\mathcal{D}_i(x; \Gamma) &\equiv -\frac{1}{2} \epsilon_{ijk} \epsilon_{klm} \mathcal{F}_{j4lm}(x; \Gamma) = -\mathbf{e}_i \langle\langle \mathbf{E}(x) \wedge \mathbf{B}(0) \rangle\rangle_{\Gamma} \\
&= -\frac{1}{2} \epsilon_{ijk} \epsilon_{klm} \mathcal{F}_{lmj4}(x; \Gamma) = -\mathbf{e}_i \langle\langle \mathbf{B}(x) \wedge \mathbf{E}(0) \rangle\rangle_{\Gamma},
\end{aligned}$$

where the fact that  $\langle\langle \mathbf{B}(x) \rangle\rangle_{\Gamma} = \mathbf{0}$  allows us to disregard some of the disconnected parts. The equalities in the last two relations are due to PT invariance. Moreover, due to T invariance, we have  $\mathcal{D}_i(\mathbf{r}, t; \Gamma) = -\mathcal{D}_i(\mathbf{r}, -t; \Gamma)$ <sup>3</sup>.

The function  $\mathcal{F}$  can be exactly expressed as a functional derivative of the Wilson loop average [7,11]:

$$\mathcal{F}_{\mu\nu\lambda\rho}(x; \Gamma) = \frac{\delta}{\delta S_{\mu\nu}(x)} \frac{\delta}{\delta S_{\lambda\rho}(0)} \log \langle W(\Gamma) \rangle. \quad (5)$$

In Refs. [7,11] the whole semirelativistic  $q\bar{q}$  potential was obtained as a gauge-invariant function of the first and second functional derivative on the logarithm of the Wilson loop. These derivatives correspond to the vacuum expectation values of one or two field strengths insertions in the static Wilson loop [8] that have been recently evaluated on the lattice [9].

Taking Eq. (3) into account, we obtain,

$$\mathcal{F}_{\mu\nu\lambda\rho}(x; \Gamma) = g^2 \langle \phi(0, x) F_{\mu\nu}(x) \phi(x, 0) F_{\lambda\rho}(0) \rangle + \mathcal{R}_{\mu\nu\lambda\rho}(x; \Gamma), \quad (6)$$

where  $\mathcal{R}$  contains all contributions from cumulants of order higher than two:

$$\begin{aligned}
\mathcal{R}_{\mu\nu\lambda\rho}(x; \Gamma) &= \sum_{n=3}^{\infty} \frac{(ig)^n}{n!} \sum_{\{\text{all perm.}(i,j)\}_{S(\Gamma)}} \int \left[ \prod_{k \neq i,j}^n dS_{\mu_k \nu_k}(u_k) \right] \\
&\times \langle \phi(0, u_1) F_{\mu_1 \nu_1}(u_1) \cdots F_{\mu\nu}(u_i = x) \cdots \\
&\times \cdots F_{\lambda\rho}(u_j = 0) \cdots F_{\mu_n \nu_n}(u_n) \phi(u_n, 0) \rangle_{\text{cum}}.
\end{aligned} \quad (7)$$

In the so-called Stochastic Vacuum Model (SVM) it is assumed that for large distances the bilocal cumulant  $\langle \phi(0, x) F_{\mu\nu}(x) \phi(x, 0) F_{\lambda\rho}(0) \rangle$  is the dominant

<sup>3</sup> For special geometries of the contour  $\Gamma$  other general properties can be derived. In particular, for a static Wilson loop we obtain  $\langle\langle E_i(x) \rangle\rangle_{\Gamma} = \frac{r_i}{r} \frac{\partial V_0(r)}{\partial r} = -\langle\langle E_i(0) \rangle\rangle_{\Gamma}$  where  $V_0(r)$  denotes the static potential between colour sources, separated by a spatial distance  $r$ . On the lattice this symmetry holds only for large  $r$ , such that we prefer to determine  $\langle\langle E_i \rangle\rangle_{\Gamma}$  by use of the relation  $\langle\langle \mathbf{E}(x) \rangle\rangle_{\Gamma} \cdot \langle\langle \mathbf{E}(0) \rangle\rangle_{\Gamma} = \lim_{t \rightarrow \infty} \langle\langle \mathbf{E}(\mathbf{r}, t) \cdot \mathbf{E}(0) \rangle\rangle_{\Gamma}$ .

contribution to  $\mathcal{F}$  in Eq. (6) [4,11,12]. Higher order cumulants are expected to be small corrections to the relevant non-perturbative parameters (like the string tension) that can be derived from the bilocal one. We have already pointed out that this assumption has been successfully tested in potential theory and soft high energy scattering (for some reviews see Ref. [4]). However, in the present work we aim at a first principles check of this assumption on the lattice. The adopted strategy is the following. Lorentz invariance is only violated by the contour  $\Gamma$  within Eq. (6). Therefore, deviations of  $\mathcal{F}$  from Lorentz invariance have to be attributed to the higher order cumulants  $\mathcal{R}$  on the right hand side. We interpret the Lorentz invariant part of the data as  $\langle \phi(0, x) F_{\mu\nu}(x) \phi(x, 0) F_{\lambda\rho}(0) \rangle$  and parameterize it in terms of two form factors. These can subsequently be compared with other lattice determinations of these quantities which have been obtained by use of the so-called cooling method [6]. We interpret deviations between our data points and continuous parameterizations as an estimate for the size of higher order corrections.

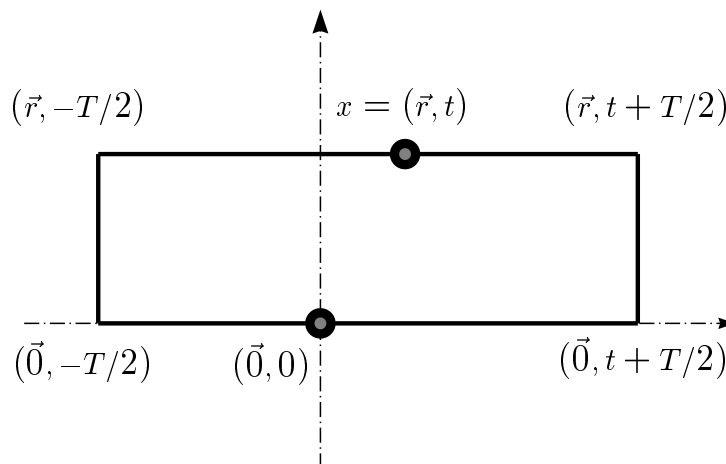


Fig. 1. *The rectangular Wilson loop  $\Gamma$  with two field strength insertions.*

Let us focus on the bilocal cumulant  $\langle \phi(0, x) F_{\mu\nu}(x) \phi(x, 0) F_{\lambda\rho}(0) \rangle$  given in Eq. (2). For our purposes it is more convenient to define the functions:

$$D_{\perp}(x^2) \equiv \frac{g^2 \langle F^2(0) \rangle}{24N_c(D(0) + D_1(0))} (D(x^2) + D_1(x^2)), \quad (8)$$

$$D_{*}(x^2) \equiv \frac{g^2 \langle F^2(0) \rangle}{24N_c(D(0) + D_1(0))} x^2 \frac{d}{dx^2} D_1(x^2). \quad (9)$$

Note that from Eq. (8) the gluon condensate is given by  $G_2 \equiv \langle g^2 F^2(0) / 4\pi^2 \rangle = D_{\perp}(0) 6N_c / \pi^2$ . The cumulant expansion Eq. (3) takes into account all perturbative as well as all non-perturbative contributions to the Wilson loop. In

particular, for what concerns the bilocal cumulant of Eq. (2), the origin of  $D$  is purely non-perturbative (with a typical behaviour  $\sim e^{-|x|/\lambda_g}$  for large  $x$ ) while  $D_1$  contains perturbative ( $\sim 1/x^4$ ) as well as non-perturbative contributions.

Some special cases of Eq. (2) are,

$$g^2 \langle \phi(0, x) F_{i4}(x) \phi(x, 0) F_{i4}(0) \rangle = 3(D_\perp(x^2) + D_*(x^2)) - 2 \frac{\mathbf{r}^2}{x^2} D_*(x^2), \quad (10)$$

$$\epsilon_{ilm} \epsilon_{ijk} g^2 \langle \phi(0, x) F_{lm}(x) \phi(x, 0) F_{jk}(0) \rangle = 12 D_\perp(x^2) + 8 \frac{\mathbf{r}^2}{x^2} D_*(x^2), \quad (11)$$

$$\epsilon_{ijk} g^2 \langle \phi(0, x) F_{i4}(x) \phi(x, 0) F_{jk}(0) \rangle = 0, \quad (12)$$

$$\epsilon_{ijk} g^2 \langle \phi(0, x) F_{jk}(x) \phi(x, 0) F_{i4}(0) \rangle = 0, \quad (13)$$

$$\epsilon_{ijk} \epsilon_{klm} g^2 \langle \phi(0, x) F_{j4}(x) \phi(x, 0) F_{lm}(0) \rangle = -4 \frac{r_i t}{x^2} D_*(x^2), \quad (14)$$

$$\epsilon_{ijk} \epsilon_{klm} g^2 \langle \phi(0, x) F_{lm}(x) \phi(x, 0) F_{j4}(0) \rangle = -4 \frac{r_i t}{x^2} D_*(x^2). \quad (15)$$

With the above definitions, we can rewrite Eq. (6) as

$$\begin{aligned} \mathcal{F}_{\mu\nu\lambda\rho}(x; \Gamma) &= (\delta_{\mu\lambda} \delta_{\nu\rho} - \delta_{\mu\rho} \delta_{\nu\lambda}) D_\perp(x^2) \\ &+ \frac{1}{x^2} (x_\mu x_\lambda \delta_{\nu\rho} - x_\mu x_\rho \delta_{\nu\lambda} + x_\nu x_\rho \delta_{\mu\lambda} - x_\nu x_\lambda \delta_{\mu\rho}) D_*(x^2) \\ &+ \mathcal{R}_{\mu\nu\lambda\rho}(x; \Gamma), \end{aligned} \quad (16)$$

and, in particular,

$$\mathcal{E}(x; \Gamma) = 3(D_\perp(x^2) + D_*(x^2)) - 2 \frac{r^2}{x^2} D_*(x^2) + \mathcal{R}_{i4i4}(x; \Gamma), \quad (17)$$

$$\mathcal{B}(x; \Gamma) = 3D_\perp(x^2) + 2 \frac{r^2}{x^2} D_*(x^2) + \frac{1}{4} \epsilon_{ilm} \epsilon_{ijk} \mathcal{R}_{lmjk}(x; \Gamma), \quad (18)$$

$$\mathcal{C}(x; \Gamma) = \frac{1}{2} \epsilon_{ijk} \mathcal{R}_{i4jk}(x; \Gamma), \quad (19)$$

$$\mathcal{D}(x, \Gamma) \equiv \frac{r_i}{r} \mathcal{D}_i(x; \Gamma) = \frac{2rt}{x^2} D_*(x^2) - \frac{1}{2} \frac{r_i}{r} \epsilon_{ijk} \epsilon_{klm} \mathcal{R}_{j4lm}(x; \Gamma). \quad (20)$$

The lattice data have been produced in order to evaluate the complete  $1/m^2$  corrections to the static quark-antiquark potential [9]. The loop  $\Gamma$  is the rectangle depicted in Fig. 1 in the limit of large separation in Euclidean time between the coordinates of the field strength insertions (ears) and the spatial closures of the Wilson loop ( $T \gg 0, t$ ). In practice, this limit has been

realized by “smearing” the spatial connections within the Wilson loop, i.e. by substituting the straight paths by a suitable linear combination of paths that maximizes the overlap with the  $q\bar{q}$  ground state (For details see Refs. [9,13]). The data have been non-perturbatively renormalized by use of the Huntley–Michael method [14].

The lattice results provide information on the functions  $\mathcal{E}$ ,  $\mathcal{B}$  and  $\mathcal{D}$ . However, not all possible choices of  $\mathcal{F}$  have been realized, such that no data on  $\mathcal{C}$  is available. In the next section we will determine the functions  $D_\perp$  and  $D_*$ , assuming that  $\mathcal{R}$  in Eqs. (17), (18) and (20) can be neglected in the Lorentz-symmetric region. Since we have more relations than functions we can also provide an independent consistency check of this assumption. In doing so we obtain two results. Firstly, as long as the data supply us with space-time symmetric functions  $D_\perp$  and  $D_*$  we can consistently assume that contributions from higher order cumulants can be neglected. In fact  $\mathcal{E}$ ,  $\mathcal{B}$  and  $\mathcal{D}$ , depending on  $\Gamma$ , are in general not space-time isotropic functions, whereas  $D_\perp$  and  $D_*$  are. On the other hand, the only source of anisotropy is  $\mathcal{R}$ . Secondly, in the region where the bilocal cumulants are established to be the dominant contributions, we obtain a parameterization of the form factors that can be compared to results already existing in the literature<sup>4</sup>.

### 3 Results

From Eqs. (17), (18) and (20) we have:

$$2rtD_*(x^2) = x^2\mathcal{D}(x; \Gamma) + \dots, \quad (21)$$

$$D_\perp(x^2) + \frac{1}{2}D_*(x^2) = \frac{1}{6}(\mathcal{B}(x; \Gamma) + \mathcal{E}(x; \Gamma)) + \dots, \quad (22)$$

$$(x^2 - 4t^2)D_*(x^2) = x^2(\mathcal{B}(x; \Gamma) - \mathcal{E}(x; \Gamma)) + \dots. \quad (23)$$

By inverting these relations we obtain  $D_*$  and  $D_\perp$  for various values of  $\mathbf{r}$  and  $t$ . In order to check space-time symmetry we will consider several combinations of  $\mathbf{r}$  and  $t$  which yield similar  $x^2 = r^2 + t^2$ . The required correlation functions  $\mathcal{E}$ ,  $\mathcal{B}$  and  $\mathcal{D}$  have been measured on the lattice in the context of the extraction of relativistic corrections to the static interquark potential [9]. The lattice simulations (with Wilson action, within the valence quark approximation to QCD) have been performed at the inverse lattice couplings  $\beta = 6.0$  and  $\beta = 6.2$  on  $16^4$  and  $32^4$  lattices, respectively. From a fit to the experimental

---

<sup>4</sup> The definition of the bilocal cumulant is not unique but depends on the set of connecting paths  $\Phi$ . However, we expect the large distance behaviour of the cumulants to be universal, in particular the correlation length.



bottomonium spectrum, we obtain inverse lattice spacings of  $a^{-1} = 2.14$  GeV and  $a^{-1} = 2.94$  GeV ( $a = 0.092$  fm and  $a = 0.067$  fm), respectively. In what follows, we will neglect systematic errors on these scale estimates from sea quark effects and higher order relativistic corrections [9].

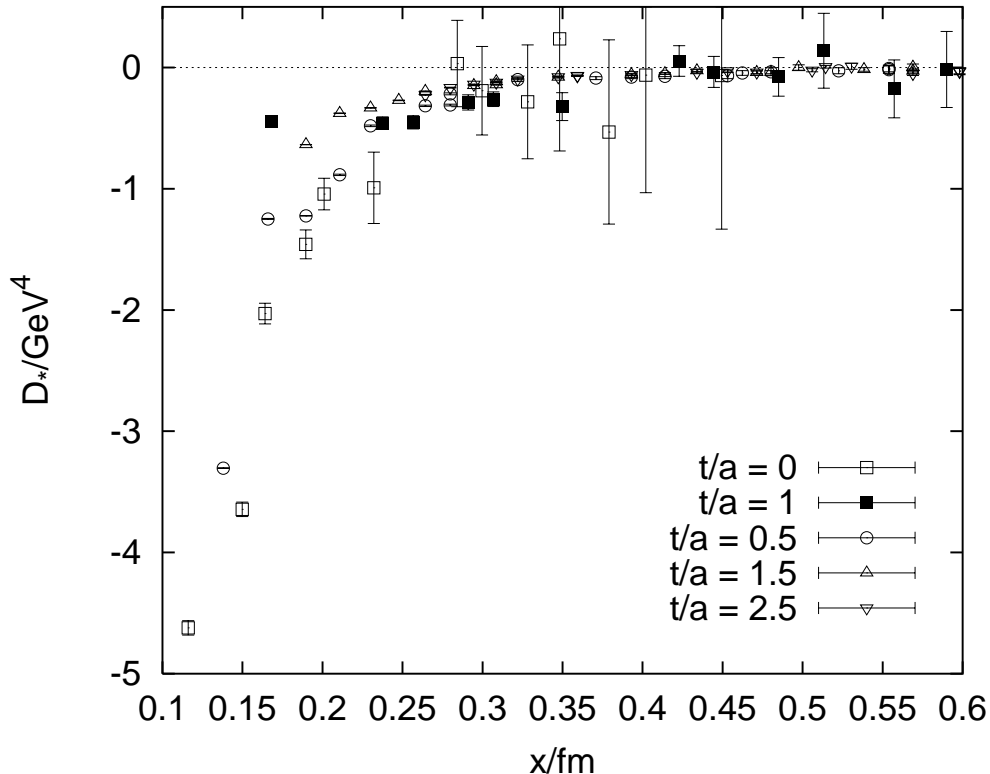


Fig. 2. Estimates of  $D_*$  from Eqs. (23) (squares) and (21) (other symbols) at  $\beta = 6.0$ .

Estimates of  $D_*$  and  $D_\perp$  from Eqs. (21)–(23) are displayed in Figs. 2 and 3, respectively. The data points at integer values of  $t/a$  in Fig. 2 have been obtained from Eq. (23) while the data at half integer values are obtained from Eq. (21). We observe that for large  $x$  all data collapse onto a universal curve. The data from Eq. (23) (squares) provides an independent consistency check with respect to Eq. (21). For small  $x$ , significant deviations from a universal curve are visible in both cases. These deviations signal that higher order cumulants become important which is simply an algebraic consequence of Eqs. (21) and (23): the function multiplying  $D_*$  in Eq. (21) vanishes for small values of  $r = \sqrt{x^2 - t^2}$  and the function multiplying  $D_*$  in Eq. (23) vanishes at the points  $x = 2t$ . For the values of  $t$  taken into account, both functions are nearly zero for small  $x$ . Therefore, in this region, contributions

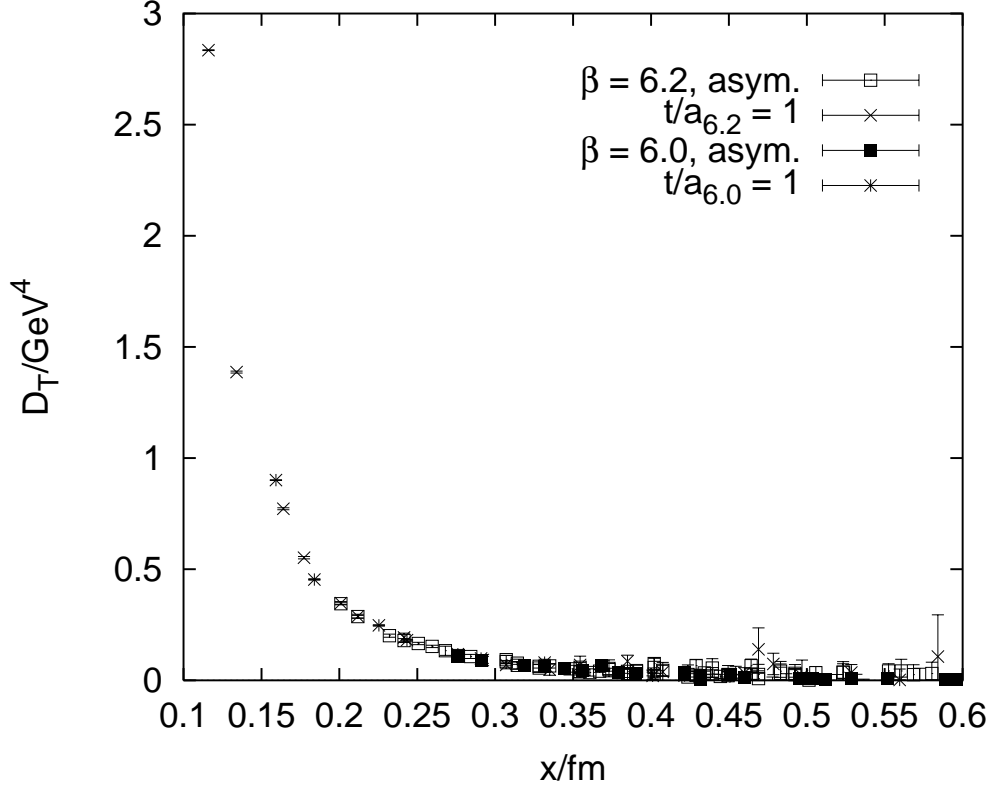


Fig. 3. Estimates of  $D_{\perp}$  from Eqs. (22) and (21) at  $\beta = 6.0$  and  $\beta = 6.2$  in comparison to the asymptotic values (squares).

of bilocal cumulants to  $\mathcal{D}$  and  $\mathcal{E} - \mathcal{B}$  are suppressed with respect to those from higher order cumulants which, as discussed above, are in general not space-time symmetric. We find that the observed behaviour is qualitatively reproduced at  $\beta = 6.2$ . In fact, data sets obtained at pairs of similar  $t$ -values (in physical units) exhibit approximate scaling, such that the data points of the figure seem to be relevant to continuum physics, rather than being mere lattice artifacts.

$D_{\perp}$  has been obtained by substituting the result on  $D_*$  from Eq. (21) (which provides us with more precise data than Eq. (23)) into Eq. (22). Contrary to the estimates on  $D_*$ , in this case deviations of data points from an asymptotic curve are small, even at small  $x$ . In Fig. 3 we display a comparison between the  $t = a$  data, obtained at  $\beta = 6.0$  and  $\beta = 6.2$ . The results do not only weakly depend on  $t$  but are almost independent of the lattice spacing  $a$ , even at these small  $t$  values.

Within the present statistical errors, universality of the curves is obtained from  $r_{\min} \geq \sqrt{5}a$  and  $t_{\min} \geq 3.5a$  ( $t_{\min} \geq 2.5a$  at  $\beta = 6.0$ ) for  $D_*(x)$  and  $r_{\min} \geq \sqrt{5}a$  and  $t_{\min} \geq 2a$  for  $D_\perp(x)$  onwards. In physical units this distance corresponds to  $x_{\min} \approx 0.3$  fm for  $D_*$  and  $x_{\min} \approx 0.2$  fm for  $D_\perp$ , respectively.

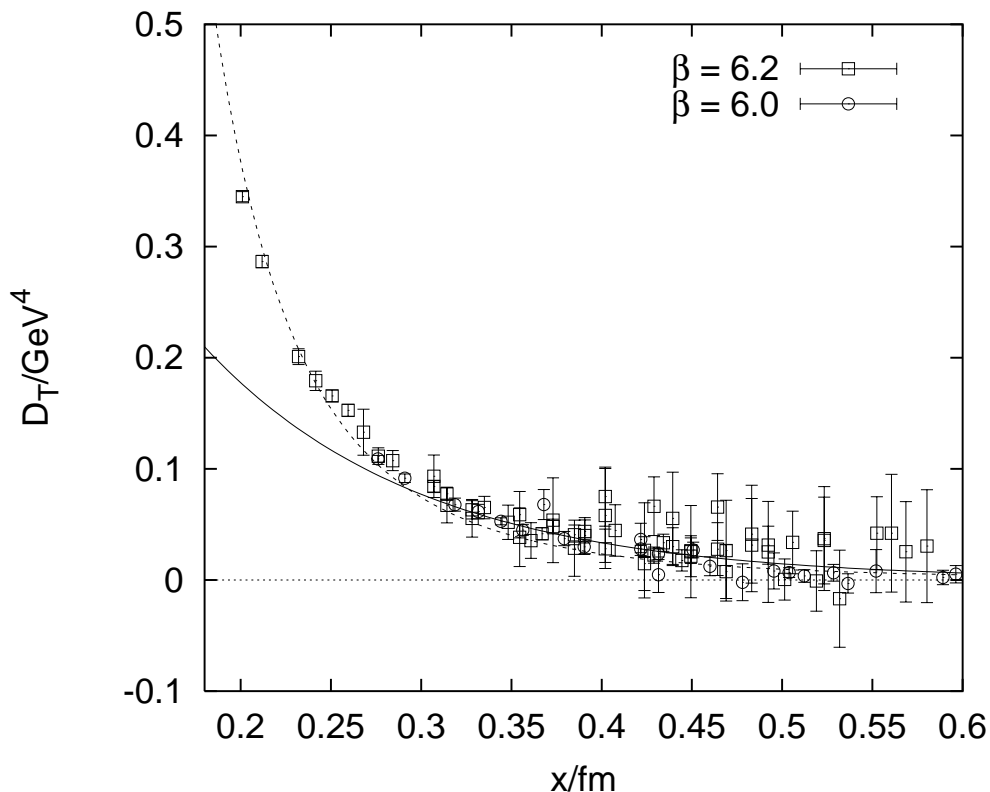


Fig. 4.  $D_\perp$  with a one exponential fit to the  $\beta = 6.0$  data (solid curve) and the curve  $0.4/x^4$  (dashed).

In Fig. 4 all asymptotic data on  $D_\perp$  is displayed, together with a one-exponential fit to the  $\beta = 6.0$  data of the form (solid line)

$$D_\perp(x^2) = A \exp(-|x|/\lambda_a), \quad (24)$$

The fit parameters remain stable for fit ranges  $x_{\min} > 0.3$  fm (see Table 1). Although even for smaller  $x_{\min}$ , exponential fits yield reasonable  $\chi^2$  values, the fit parameters turn out to be unstable under variation of the fit range. Within errors the parameters obtained at the two lattice spacings agree with each other. We quote as a final result the more precise value obtained at  $\beta = 6.0$ ,

$$\lambda_a = 0.120^{+0.009}_{-0.012} \text{ fm}. \quad (25)$$

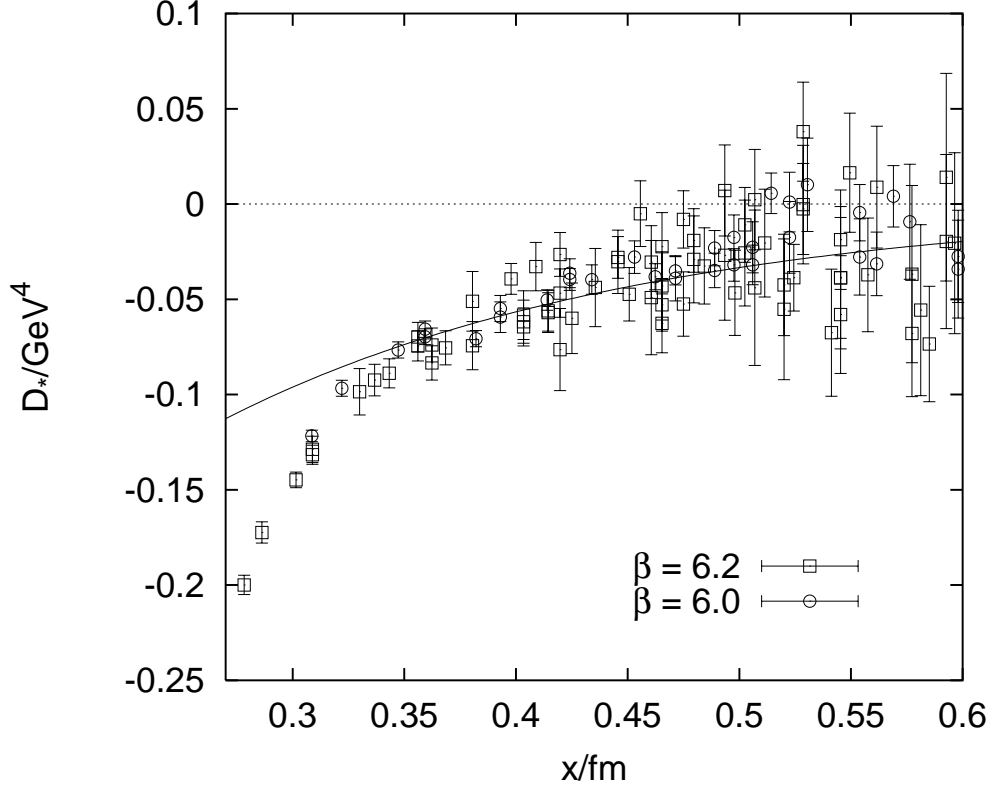


Fig. 5.  $D_*$  with a one exponential fit to the  $\beta = 6.0$  data.

Table 1  
Fits to  $D_\perp$ .

$\beta$	$x_{\min}/a$	$\lambda_a/\text{fm}$	$A/\text{GeV}^4$	$\chi^2/N_{DF}$
6.0	3.46	$0.120^{+09}_{-12}$	$0.94^{+32}_{-16}$	0.68
6.2	4.69	$0.153^{+22}_{-35}$	$0.56^{+47}_{-15}$	0.80

In addition, a curve  $c/x^4$ , which is the functional form one would expect from perturbation theory, with  $c = 0.4$  is plotted in order to show the dominance of the perturbative regime in the short range region.

In Fig. 5 the asymptotic data on  $D_*$  is plotted, together with an exponential fit of the form

$$D_*(x^2) = -B \exp(-|x|/\lambda_b), \quad (26)$$

to the  $\beta = 6.0$  data. The fit parameters remain stable for fit ranges  $x_{\min} > 0.35$

Table 2  
Fits to  $D_*$ .

$\beta$	$x_{\min}/a$	$\lambda_b/\text{fm}$	$B/\text{GeV}^4$	$\chi^2/N_{DF}$
6.0	3.77	$0.189^{+13}_{-29}$	$0.47^{+20}_{-06}$	1.25
6.2	4.92	$0.249^{+16}_{-54}$	$0.33^{+17}_{-04}$	1.47

fm (see Table 2). Again, within errors the parameters obtained at the two lattice agree with each other. We end with the  $\beta = 6.0$  estimate,

$$\lambda_b = 0.189^{+0.013}_{-0.029} \text{ fm.} \quad (27)$$

Note that  $\lambda_a$  and  $\lambda_b$  are lower limits on the corresponding asymptotic correlation length(s) while  $A$  and  $B$  are upper limits on the asymptotic amplitudes.

## 4 Conclusions

In this letter we have shown that the lattice data for the long range behaviour of the two-field strength insertion on a rectangular Wilson loop are compatible with a two point cumulant approximation. This approximation is crucial in the so-called Stochastic Vacuum Model of QCD. Moreover our data are compatible with an exponential fit  $\sim e^{-|x|/\lambda_g}$  with a gluonic correlation length  $\lambda_g$  of around 0.1–0.2 fm. These findings are in agreement with the quenched results obtained in [6] by means of lattice simulations with the cooling method. In general one might expect the cooling method, that removes short range fluctuations, to have the tendency of underestimating masses and thus to overestimate correlation lengths. On the other hand our results are more sensitive to the perturbative regime which certainly dominates the region in which the exponential curves of Fig. 4 and Fig. 5 deviate from the data (typically for distances shorter than 0.3 fm). For the moment being, our data suffer under much bigger statistical errors than those obtained after cooling. This is natural since we do not cut off short range fluctuations. However, we obtain first independent estimates of the form factors. Unlike cooling, the Huntley–Michael lattice renormalization does not affect transfer matrix elements. Moreover, it has been checked [9] against the exact continuum Gromes [15] and Barchielli–Brambilla–Prosperi [8] relations. Another advantage of the present method is that the two point cumulant has been extracted from quantities that have a direct physical interpretation and play a role in heavy quarkonia spectroscopy. We have shown that an evaluation of the bilocal cumulant from existing lattice data is possible with the proposed method. We expect that in the near future more selective fits can be performed on more precise data.

**Acknowledgments** G. B. has been supported by DFG grant No. Ba 1564/3-1 and PPARC grant No. GR/K55738. He expresses thanks to his collaborators Armin Wachter and Klaus Schilling. N. B. is pleased to acknowledge useful discussions with A. Di Giacomo. Computations have been performed on the Connection Machines CM-5 of the Institut für Angewandte Informatik in Wuppertal and the GMD in St. Augustin. We appreciate support from the EU (grant Nos. SC1\*-CT91-0642 and CHRX-CT92-00551) and the Deutsche Forschungsgemeinschaft (DFG grant Nos. Schi 257/1-4 and Schi 257/3-2).

## References

- [1] M. A. Shifman, A. I. Vainshtein and V. I. Zakharov, Nucl. Phys. **B147**, 385 (1979).
- [2] D. Gromes, Phys. Lett. **B115**, 482 (1982).
- [3] H. G. Dosch, Phys. Lett. **B190**, 177 (1987); H. G. Dosch and Yu. A. Simonov, Phys. Lett. **B205**, 339 (1988).
- [4] H. G. Dosch, Prog. Part. Nucl. Phys. **33**, 121 (1994); H. G. Dosch in Proceedings of the Int. School E. Fermi, Course CXXX, Varenna 1995; O. Nachtmann, Lectures given at the International University School of Nuclear and Particle Physics Schladming, Austria, (1996) HD-THEP-96-38.
- [5] L. Del Debbio, A. Di Giacomo, Yu. A. Simonov, Phys. Lett. **B332**, 111 (1994).
- [6] M. D'Elia, A. Di Giacomo and E. Meggiolaro, Phys. Lett. **B408**, 315 (1997); M. Campostrini, A. Di Giacomo and G. Mussardo, Z. Phys. **C25**, 173 (1984); A. Di Giacomo and H. Panagopoulos Phys. Lett. **B285**, 133 (1992); A. Di Giacomo, E. Meggiolaro and H. Panagopoulos, Nucl. Phys. **B483**, 371 (1997).
- [7] N. Brambilla, P. Consoli and G. M. Prosperi, Phys. Rev. **D50**, 5878 (1994).
- [8] A. Barchielli, N. Brambilla and G. M. Prosperi, Nuovo Cimento **103A**, 59 (1990); A. Barchielli, E. Montaldi and G. M. Prosperi, Nucl. Phys. **B296**, 625 (1988).
- [9] G. S. Bali, K. Schilling and A. Wachter, Phys. Rev. **D56**, 2566 (1997).
- [10] N. G. Van Kampen, Phys. Rep. **24C**, 171 (1976).
- [11] N. Brambilla and A. Vairo, Phys. Rev. **D55**, 3974 (1997); M. Baker, J. Ball, N. Brambilla and A. Vairo, Phys. Lett. **B389**, 577 (1996).
- [12] Yu. A. Simonov, Nucl. Phys. **B307**, 512 (1988); **B324**, 67 (1989).
- [13] G. S. Bali, K. Schilling and A. Wachter, Phys. Rev. **D55**, 5309 (1997).
- [14] A. Huntley and C. Michael, Nucl. Phys. **B286**, 211 (1987).
- [15] D. Gromes, Z. Phys. **C26**, 401 (1984).